Resolving Nonclassical Magnon Composition of a Magnetic Ground State via a Qubit

Anna-Luisa E. Römling,* Alejandro Vivas-Viaña, Carlos Sánchez Muñoz, and Akashdeep Kamra
Condensed Matter Physics Center (IFIMAC) and Departamento de Física Teórica de la Materia Condensada, Universidad Autónoma de Madrid, E-28049 Madrid, Spain

(Received 8 June 2023; accepted 29 August 2023; published 3 October 2023)

Recently gained insights into equilibrium squeezing and entanglement harbored by magnets point toward exciting opportunities for quantum science and technology, while concrete protocols for exploiting these are needed. Here, we theoretically demonstrate that a direct dispersive coupling between a qubit and a noneigenmode magnon enables detecting the magnonic number states' quantum superposition that forms the ground state of the actual eigenmode—squeezed magnon—via qubit excitation spectroscopy. Furthermore, this unique coupling is found to enable control over the equilibrium magnon squeezing and a deterministic generation of squeezed even Fock states via the qubit state and its excitation. Our work demonstrates direct dispersive coupling to noneigenmodes, realizable in spin systems, as a general pathway to exploiting the equilibrium squeezing and related quantum properties thereby motivating a search for similar realizations in other platforms.

DOI: 10.1103/PhysRevLett.131.143602

Introduction.—Quantum superposition is a central concept and ingredient underlying diverse phenomena from entanglement to the quantum speedup in computing [1,2]. A bosonic mode, such as a photon, can be driven into a so-called nonclassical superposition of its eigenstates—number or Fock states—thereby admitting various quantum advantages [3,4], such as enhancement in its coupling to a qubit via squeezing [5–9]. At the same time, engineering a dispersive effective interaction $\sim\hat{c}^\dagger\hat{c}\hat{\sigma}_z$ between the boson (annihilation operator $\hat{c}$) and the qubit $\hat{\sigma}_z$ leads to the latter's excitation frequency becoming multivalued and providing information on the boson's wave function [10–12]. This has been exploited to measure the quantum superposition of the number states that constitutes a given bosonic state [10,12–16]. Since such bosons are also the interconnects in quantum computers, this interplay between their nonclassical states and qubits bears a high relevance for emerging quantum technologies [2,17].

The bosonic spin excitations of magnets, broadly called magnons, potentially offer advantages in realizing quantum properties [15,18–20]. Magnets have been shown to naturally harbor nonclassical squeezed states in *equilibrium* [21] arising from an interplay between energy minimization and the Heisenberg uncertainty principle [18,19,28]. For example, the ground state and eigenmodes of an anisotropic ferromagnet are constituted by nonclassical superpositions of states with different number of spin flips or, equivalently, magnons [18,34]. The latter are not the eigenmodes but represent the natural or physical basis for the magnet. Hence, the question arises if and how one can measure such nonclassical superpositions of noneigenmode basis states that constitute the system eigenmodes. An answer to this is also desirable for harnessing the concomitant *equilibrium* entanglement harbored by these spin systems for useful quantum information tasks.

In this Letter, taking inspiration from the successful detection of nonequilibrium nonclassical superpositions via a qubit [10,13–16] and building upon recent advances in probing magnets via qubits [13,15,16,35–40], we address the question posed above. We theoretically demonstrate a protocol for measuring the intrinsic nonclassical superposition that forms the squeezed-magnon vacuum ground state of an anisotropic ferromagnet. We find that the conventional qubit spectroscopy employing a coherent qubit-magnon coupling [10,11,41] fails in this goal. However, we show that achieving a direct dispersive interaction (Fig. 1) between the qubit and the noneigenmode magnon is the key to achieving this goal. Such a coupling may result from, e.g., the exchange interaction between the magnet and a spin qubit [42,43]. Furthermore, our proposed qubit-magnon coupling enables a deterministic protocol to generate nonequilibrium squeezed even Fock states [44,45] by driving the qubit at specific frequencies (Fig. 2).

Direct dispersive coupling between magnon and qubit.—We consider a ferromagnetic insulator with its equilibrium spin order along the z axis and a spatially uniform (wave vector $\boldsymbol{k}=\boldsymbol{0}$) magnonic mode, represented by the annihilation operator $\hat{a}$. The ferromagnet is coupled to a spin qubit, represented by the operator $\hat{\sigma}_z$, via a spin-spin interaction such as dipolar or exchange coupling (Fig. 1) [46–50]. The $\hat{S}_z\hat{\sigma}_z$ contribution of the spin-spin interaction provides a direct dispersive coupling $\sim\hat{a}^\dagger\hat{a}\hat{\sigma}_z$ [see Supplemental Material (SM) [51]]. For the moment, we disregard any coherent coupling returning to it later. Because of magnetic anisotropy in the x-y plane, magnons are not the eigenexcitations [28,47] and the total Hamiltonian reads ($\hbar=1$)

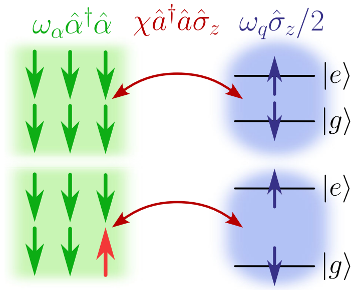

FIG. 1. Schematic depiction of the system. The bosonic uniform magnon mode in a ferromagnet (FM, green) is coupled to a spin qubit (blue) through a spin-spin (e.g., exchange) interaction. The ferromagnetic eigenmode is squeezed magnon $\hat{\alpha}$, while the qubit $\hat{\sigma}_z$ interacts dispersively with the spin flip or magnon $\hat{a}$ via $\chi\hat{\sigma}_z\hat{a}^\dagger\hat{a}$. This direct dispersive coupling originates from the qubit energy depending on the total FM spin, which is governed by the number of spin flips or magnons (compare upper and lower panels).

$$\hat{\mathcal{H}}_{\mathrm{syst}} = A\hat{a}^\dagger\hat{a} + B\hat{a}^2 + B^*\hat{a}^{\dagger 2} + \frac{\omega_q}{2}\hat{\sigma}_z + \chi\hat{a}^\dagger\hat{a}\hat{\sigma}_z, \quad (1)$$

where A and B parametrize the anisotropic ferromagnet [47] with B resulting from the x-y plane anisotropy, ω_q is the excitation energy of the uncoupled qubit, and χ (assumed positive here) is the direct dispersive coupling strength. A derivation of Eq. (1) is presented in the SM [51].

The ferromagnet only part of the Hamiltonian in Eq. (1) can be diagonalized to $\omega_\alpha\hat{\alpha}^\dagger\hat{\alpha}$ with $\hat{\alpha} = \hat{a}\cosh r + \hat{a}^\dagger \sinh r e^{i\theta}$ [28,47] and

$$\omega_\alpha = \sqrt{A^2 - 4|B|^2}, \quad (2)$$

$$2r = \operatorname{arctanh}\left(\frac{2|B|}{A}\right). \quad (3)$$

We refer to the eigenmode $\hat{\alpha}$ as bare squeezed magnon, since it is related to the magnon $\hat{a}$ via the single-mode squeeze operator [3,28,47]. The squeezing variables r and θ are determined by A and B of Eq. (1) (see SM [51] for further details), noting that squeezing and r vanish for $B = 0$. As a result, the ferromagnet ground state is vacuum of the squeezed magnon $\hat{\alpha}$, which is formed by a quantum superposition of the even magnon $\hat{a}$ number states [18,19]. Since the $\hat{a}$ magnons are not the eigenmodes, it is not clear how to detect this nonclassical superposition.

Magnon number dependent qubit excitation energy.—The nonequilibrium superpositions of eigenmode number states have been investigated via measurement of multiple peaks in a qubit excitation spectroscopy [10,12,14]. Here, each peak comes from a different number state contribution to the superposition. Despite a similar motivation, this should be clearly contrasted with our goal and challenge of resolving the noneigenmode magnon number state composition of the equilibrium or eigenmode state—the squeezed-magnon vacuum [18,19,28]. We hypothesize that the desired resolution can be accomplished in our considered model (Fig. 1) when the qubit energy depends directly on the noneigenmode magnon number ($\sim\chi\hat{a}^\dagger\hat{a}\hat{\sigma}_z$), by spectroscopically probing the qubit excitation energies. We now evaluate the latter to examine this hypothesis.

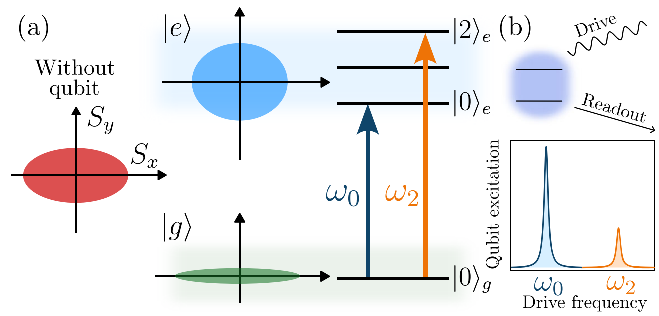

FIG. 2. Qubit excitation spectroscopy of squeezed-magnon vacuum. (a) The ferromagnet hosts equilibrium-squeezed magnons and corresponding vacuums. As a result, the zero-point quantum fluctuations depicted in the spin phase space bear elliptical profiles [18], indicative of their squeezing. The degree of squeezing is different in three cases: (i) qubit not coupled to the FM (red), (ii) qubit in excited state $|e\rangle$ (blue), and (iii) qubit in ground state $|g\rangle$ (green). When one spectroscopically probes the qubit excitation energy ($|g\rangle \to |e\rangle$), the squeezed-magnon number can change from 0 to any number state available in the superposition, due to the differing magnon squeezings in the qubit excited and ground states. (b) This effectively allows us to probe the squeezed-magnon vacuum as a superposition of *even* magnon number states, with each peak (only first two depicted here) in the qubit excitation spectroscopy measuring a term in the superposition.

We first project the total Hamiltonian Eq. (1) onto the qubit ground state $|g\rangle$. The reduced Hamiltonian $\hat{\mathcal{H}}_g = \langle g|\hat{\mathcal{H}}_{\mathrm{syst}}|g\rangle$ is obtained as

$$\hat{\mathcal{H}}_g = (A-\chi)\hat{a}^\dagger\hat{a} + B\hat{a}^2 + B^*\hat{a}^{\dagger 2} - \frac{\omega_q}{2}. \quad (4)$$

In a direct analogy with the discussion and analysis following Eq. (1), the reduced Hamiltonian Eq. (4) can be diagonalized to $\omega_\alpha^g\hat{\alpha}_g^\dagger\hat{\alpha}_g$ with a different squeezed-magnon $\hat{\alpha}_g$ eigenmode characterized by a frequency $\omega_\alpha^g < \omega_\alpha$ and squeezing factor $r_g > r$. ω_α^g and r_g are obtained from Eqs. (2) and (3) by substituting $A \to A - \chi$ [67]. We will refer to $\hat{\alpha}_g$ as the ground state squeezed magnon harboring a different magnetic vacuum as compared to the isolated ferromagnet [Fig. 2(a)]. The projection $\hat{\mathcal{H}}_e = \langle e|\hat{\mathcal{H}}_{\mathrm{syst}}|e\rangle$ onto the qubit excited state $|e\rangle$ can be obtained from Eq. (4) by changing the sign of χ and ω_q. Analogous to the discussion above, the bosonic eigenmode of $\hat{\mathcal{H}}_e$ becomes the excited state squeezed magnon $\hat{\alpha}_e$ characterized by eigenenergy $\omega_\alpha^e > \omega_\alpha$ and squeezing factor $r_e < r$

[Fig. 2(a)], with ω_α^e and r_e obtained from Eqs. (2) and (3) on replacing $A \to A + \chi$.

Altogether, we have diagonalized our Hamiltonian Eq. (1) denoting the eigenstates by $|n\rangle_e$ and $|n\rangle_g$, where the subscript g or e indicates the qubit state and $n \in \mathbb{N}$ labels the different Fock states. The key point is that the magnonic eigenmodes and their respective squeezing are different in three cases: (i) isolated ferromagnet, (ii) qubit in its ground state, and (iii) qubit in its excited state [see Fig. 2(a)].

The typical qubit excitation spectroscopy measures qubit energy corresponding to the transition $|g\rangle \to |e\rangle$, while the boson number state remains the same [10,11]. Consequently, when we have a nonequilibrium superposition of multiple number states, the result is observation of boson number-dependent qubit energy that manifests itself as multiple spectroscopy peaks. In sharp contrast, our system has a boson mode whose squeezing depends on the qubit state. Hence, the excitation of qubit need not preserve the boson number. Thus, transitions $|0\rangle_g \to |n\rangle_e$ will take place with probability $p_n = |c_n|^2 \equiv |_e\langle n|0\rangle_g|^2$ resulting in correspondingly high spectroscopy peaks. As demonstrated in the SM [51], the ground state $|0\rangle_g$ is squeezed with respect to the excited state squeezed-magnon vacuum $|0\rangle_e$ with effective squeezing factor of $r_{\text{eff}} = r_g - r_e$ [Eq. (3)]. Thus, we may express $|0\rangle_g = \sum_n c_n |n\rangle_e$ with [3,4]

$$c_{2n} = \frac{1}{\sqrt{\cosh r_{\text{eff}}}} (-e^{i\theta} \tanh r_{\text{eff}})^n \frac{\sqrt{(2n)!}}{2^n n!} \tag{5}$$

and $c_{2n+1} = 0$ for $n \in \mathbb{N}$. To summarize, the qubit spectroscopy should yield a peak for each of the superposition contributions [Fig. 2(b)], as intuitively hypothesized above. However, it resolves the ground state squeezed-magnon vacuum $|0\rangle_g$ in terms of the excited state squeezed-magnon number states $|n\rangle_e$ [Eq. (5)].

In Fig. 3(a), we plot the squeezing factors r_g, r_e, and r_{eff} as a function of the dispersive coupling strength χ. Only at a certain value of χ, r_{eff} is equal to the squeezing r of the bare squeezed magnon. In this case, the spectroscopy would probe the "true" distribution of the bare squeezed-magnon $\hat{\alpha}$ vacuum in terms of the magnon $\hat{a}$ Fock states. Nevertheless, employing our analysis above, a knowledge of χ and ω_α allows one to translate an observed superposition into any desired basis.

We now examine the position of the spectroscopy peaks. As per energy conservation, the transition $|0\rangle_g \to |2n\rangle_e$ occurs when the drive frequency matches the energy difference between the two states. As detailed in the SM [51], this is evaluated as ω_{2n}

$$\omega_{2n} = \omega_q + \frac{\omega_\alpha^e - \omega_\alpha^g}{2} - \chi + 2n\,\omega_\alpha^e. \tag{6}$$

For $\chi \ll \min[|A|, ||B|(A/2|B| - 2|B|/A)|]$, Eq. (6) becomes $\omega_{2n} \approx \omega_q + 2\chi \sinh^2 r + 2n[\omega_\alpha + \chi \cosh(2r)]$. The different peaks are now well separated by multiples of the bare squeezed-magnon frequency ω_α, potentially making them easier to detect [68].

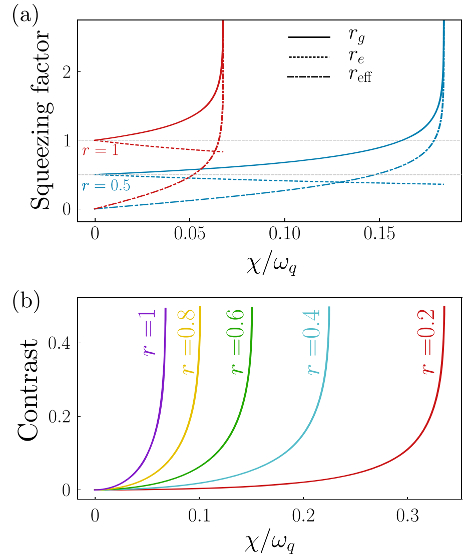

FIG. 3. (a) Squeezing factors vs χ for the magnonic eigenmodes in the qubit ground state r_g (solid line), the qubit excited r_e (dotted line), and effective squeezing $r_{\text{eff}} = r_g - r_e$ (dashed line) considering bare magnon squeezing of $r = 0.5$ (blue) and $r = 1$ (red). (b) Contrast $c = p_2/p_0$ [Eq. (7)] as a function of χ for several values of the squeezing factor r. Its vanishing in the limit $r \to 0$ signifies that more than one peak in the spectroscopy is observed only for nonzero magnon squeezing. We consider $\omega_\alpha/\omega_q = 0.5$ here.

In order to guide and quantify the measurability of multiple peaks resulting from the superpositions, we define "contrast" as the ratio $c = p_2/p_0$ evaluating it as

$$2c = \tanh^2(r_{\text{eff}}). \tag{7}$$

The contrast c, plotted in Fig. 3(b), generally characterizes the reduction of subsequent peaks expected in the qubit spectroscopy. For small coupling strengths $|\chi| \ll \min[|A|, |A(A/2|B| - 2|B|/A)|]$, we obtain $c \approx 2|B|^2\chi^2/(A^2 - 4|B|^2)^2$. For small $|B| \ll \min[|A-\chi|, |A+\chi|]$ and thus squeezing, the contrast can be expanded as $c \approx 2\chi^2|B|^2/(A^2 - \chi^2)^2$. Thus, the equilibrium superposition peaks can be observed in the qubit spectroscopy when both the direct dispersive interaction strength χ and squeezing r are nonzero, with the resolvability of the peaks increasing with both these parameters.

Simulation of qubit spectroscopy.—We now corroborate and complement our analytic considerations above by simulating a qubit spectroscopy setup using the QuTip package [69,70]. While different experimental methods can be employed to probe the qubit excitation energy [10,14], here we consider a microwave qubit drive described by $\hat{\mathcal{H}}_\text{d} = \Omega_d \cos(\omega_d t)(\hat{\sigma}_+ + \hat{\sigma}_-)$, where Ω_d denotes the Rabi frequency quantifying the drive strength, while ω_d becomes the drive frequency. As detailed in the SM [51], we consider Eq. (1) and $\hat{\mathcal{H}}_d$ to describe our system and account for qubit dissipation [71] via one collapse operator $\hat{C} = \sqrt{\gamma_q}\hat{\sigma}_-$ with qubit decay rate γ_q. Solving the Lindblad master equation [71–73] numerically, we investigate the steady state qubit excitation $\langle\hat{\sigma}_+\hat{\sigma}_-\rangle$. Ω_d is chosen small enough (see SM [51] for a quantification of this smallness) for the qubit excitation to remain small and in the linear regime [51,71]. With this protocol, the qubit excitation should manifest a peak whenever the drive frequency ω_d is resonant with a qubit excitation transition.

In Fig. 4, we show simulations (solid curves) of the qubit spectroscopy for two squeezing factors $r = 0.2$ and $r = 0.45$, comparing them with our analytic results plotted as bars at $\omega_d = \omega_{2n}$ [Eq. (6)] with heights $\propto p_{2n} = |c_{2n}|^2$ [Eq. (5)]. Thus, our analytics agree well with the simulations. We therefore conclude that the first nontrivial peak indeed stems from the equilibrium squeezing. Because of a large separation ($\sim\omega_\alpha$) between the peaks, experiments may further employ higher values of the drive Ω_d in measuring the smaller peaks. We demonstrate this point explicitly by simulating the ω_4 peak in SM [51].

Consideration of coherent coupling.—Until now, we have considered a magnet coupled to a spin qubit that offers a direct dispersive coupling χ [Eq. (1)], found to be essential for the key phenomena addressed here. We now examine the role of coherent or Rabi interaction [74] parametrized by g, such that the system Hamiltonian becomes

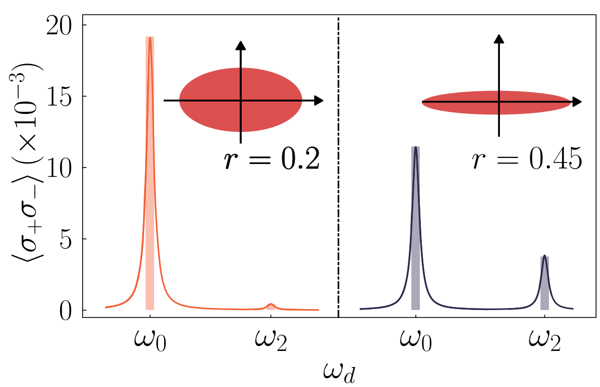

FIG. 4. Numerical simulation of qubit spectroscopy using a Rabi drive. Steady state qubit excitation $\langle\hat{\sigma}_+\hat{\sigma}_-\rangle$ is plotted against the Rabi drive frequency ω_d for two different values of bare magnon squeezing r. The first two qubit excitation frequencies ω_0 and ω_2 are observed. The shaded bars depict the analytically evaluated excitation distributions [Eqs. (5) and (6)], underlining their good agreement with the simulations. Parameters employed in the simulation are $\omega_\alpha/\omega_q = 0.5$, $\chi/\omega_q = 0.2$, $\gamma_q/\omega_q = 0.1$, and $\Omega_d/\omega_q = 0.014$. The numerical method is detailed in the SM [51].

$$\hat{\mathcal{H}}_{\mathrm{syst,SC}} = A\hat{a}^\dagger\hat{a} + B\hat{a}^2 + B^*\hat{a}^{\dagger 2} + \frac{\omega_q}{2}\hat{\sigma}_z + g(\hat{a}^\dagger + \hat{a})(\hat{\sigma}_+ + \hat{\sigma}_-). \tag{8}$$

This interaction is universally present in qubits, such as with spin [42,43] and superconducting (SC) qubits [40,41,75], while the direct dispersive coupling is not always available. When the boson and qubit are strongly detuned, i.e., $g \ll |\omega_q - \omega_\alpha|$, the coherent coupling also results in an effective dispersive interaction $\sim\tilde{\chi}\hat{\alpha}^\dagger\hat{\alpha}\hat{\sigma}_z$ [3,10,11,51,76] which has been exploited in observing nonequilibrium superpositions in terms of the eigenmode number states. It is not clear whether one can employ this effective dispersive coupling to resolve an equilibrium superposition.

Via numerical simulations of qubit spectroscopy employing Eq. (8) (see SM [51]), we find that the effective dispersive interaction $\sim\tilde{\chi}\hat{\alpha}^\dagger\hat{\alpha}\hat{\sigma}_z$ does not resolve the nonclassical magnon composition of the equilibrium squeezed-magnon vacuum. This can be understood *a posteriori* since such an effective coupling may address only the eigenmodes $\hat{\alpha}$, and not any internal noneigenmodes. Thus, a direct dispersive interaction $\sim\chi\hat{a}^\dagger\hat{a}\hat{\sigma}_z$ offered by, e.g., a spin qubit is needed for resolving equilibrium superpositions. We also show that any influence of the coherent coupling g when employing a spin qubit system can be suppressed via an adequately large detuning $|\omega_q - \omega_\alpha|$ [51,76].

Discussion.—In the conventional qubit spectroscopy for dispersively sensing a nonequilibrium quantum superposition of eigenmode Fock states, the peaks are separated in frequency by $\sim\tilde{\chi}$, which is typically small [10–12]. In our demonstrated protocol for detecting the equilibrium superposition of noneigenmode Fock states, the corresponding peaks are well separated $\sim\omega_\alpha$, which makes it feasible to detect them [77] even when they are relatively small (see SM [51]).

The direct dispersive interaction results from the $\hat{S}_z\hat{\sigma}_z$ term contained in exchange as well as dipolar spin-spin interaction hosted by multiple magnet–spin qubit platforms, as discussed in SM [51]. The resulting χ offered by an exchange-coupled spin qubit can be large ~GHz for small size of the magnet (see the SM [51]) making our proposal better suited for nanomagnets. Furthermore, detection of the nth nontrivial peak in the qubit spectroscopy is accompanied by the transition $|0\rangle_g \to |2n\rangle_e$ which provides a new deterministic approach to generate nonequilibrium squeezed Fock states [$|2n\rangle_e = S^{-1}(r_{\mathrm{eff}})|2n\rangle_g$ [18,28,44,45]] by driving the qubit.

Conclusion.—We have theoretically demonstrated how a direct dispersive interaction between a qubit and a noneigenmode boson (here, a magnon) enables detection of the quantum superposition that makes up the actual eigenmodes (here, squeezed magnon and its vacuum). The same coupling is shown to allow for a control of the equilibrium magnon squeezing and a deterministic generation of squeezed even Fock states via the qubit state and its resonant excitation. Thus, this direct dispersive interaction, readily available in spin systems, opens new avenues for exploiting the equilibrium squeezing and entanglement harbored by magnets. At the same time, our work inspires a search for the realization of direct dispersive interaction in other, such as optical [78] and mechanical, platforms that could enable access to equilibrium superpositions.

We thank Frank Schlawin for valuable discussions. We acknowledge financial support from the Spanish Ministry for Science and Innovation—AEI Grant No. CEX2018-000805-M (through the "Maria de Maeztu" Programme for Units of Excellence in R&D) and Grant No. RYC2021-031063-I funded by MCIN/AEI and "European Union Next Generation EU/PRTR". A.-L. E. R. acknowledges that the project that gave rise to these results received the support of a fellowship from "la Caixa" Foundation (ID 100010434), with fellowship code LCF/BQ/DI22/11940029. C. S. M. acknowledges that the project that gave rise to these results received the support of a fellowship from "la Caixa" Foundation (ID 100010434) and from the European Union's Horizon 2020 research and innovation programme under the Marie Skłodowska-Curie Grant Agreement No. 847648, with fellowship code LCF/BQ/PI20/11760026, and financial support from the MCINN project PID2021-126964OB-I00 (QENIGMA) and the Proyecto Sinérgico CAM 2020 Y2020/TCS-6545 (NanoQuCo-CM).

*anna-luisa.romling@uam.es

[1] S. Wehner, D. Elkouss, and R. Hanson, Quantum internet: A vision for the road ahead, Science **362**, eaam9288 (2018).
[2] A. Laucht *et al.*, Roadmap on quantum nanotechnologies, Nanotechnology **32**, 162003 (2021).
[3] C. Gerry, P. Knight, and P. L. Knight, *Introductory Quantum Optics* (Cambridge University Press, Cambridge, England, 2005).
[4] *Quantum Optics*, edited by D. Walls and G. J. Milburn (Springer, Berlin, 2008).
[5] D. F. Walls, Squeezed states of light, Nature (London) **306**, 141 (1983).
[6] C. Leroux, L. C. G. Govia, and A. A. Clerk, Enhancing Cavity Quantum Electrodynamics via Antisqueezing: Synthetic Ultrastrong Coupling, Phys. Rev. Lett. **120**, 093602 (2018).
[7] W. Qin, A. Miranowicz, P.-B. Li, X.-Y. Lü, J. Q. You, and F. Nori, Exponentially Enhanced Light-Matter Interaction, Cooperativities, and Steady-State Entanglement Using Parametric Amplification, Phys. Rev. Lett. **120**, 093601 (2018).
[8] S. C. Burd, R. Srinivas, H. M. Knaack, W. Ge, A. C. Wilson, D. J. Wineland, D. Leibfried, J. J. Bollinger, D. T. C. Allcock, and D. H. Slichter, Quantum amplification of boson-mediated interactions, Nat. Phys. **17**, 898 (2021).
[9] S. Zeytinoğlu, A. İmamoğlu, and S. Huber, Engineering Matter Interactions Using Squeezed Vacuum, Phys. Rev. X **7**, 021041 (2017).
[10] D. I. Schuster, A. A. Houck, J. A. Schreier, A. Wallraff, J. M. Gambetta, A. Blais, L. Frunzio, J. Majer, B. Johnson, M. H. Devoret, S. M. Girvin, and R. J. Schoelkopf, Resolving photon number states in a superconducting circuit, Nature (London) **445**, 515 (2007).
[11] M. Boissonneault, J. M. Gambetta, and A. Blais, Dispersive regime of circuit QED: Photon-dependent qubit dephasing and relaxation rates, Phys. Rev. A **79**, 013819 (2009).
[12] R. Bianchetti, S. Filipp, M. Baur, J. M. Fink, M. Göppl, P. J. Leek, L. Steffen, A. Blais, and A. Wallraff, Dynamics of dispersive single-qubit readout in circuit quantum electrodynamics, Phys. Rev. A **80**, 043840 (2009).
[13] D. Lachance-Quirion, Y. Tabuchi, S. Ishino, A. Noguchi, T. Ishikawa, R. Yamazaki, and Y. Nakamura, Resolving quanta of collective spin excitations in a millimeter-sized ferromagnet, Sci. Adv. **3**, e1603150 (2017).
[14] S. Kono, Y. Masuyama, T. Ishikawa, Y. Tabuchi, R. Yamazaki, K. Usami, K. Koshino, and Y. Nakamura, Nonclassical Photon Number Distribution in a Superconducting Cavity under a Squeezed Drive, Phys. Rev. Lett. **119**, 023602 (2017).
[15] D. Lachance-Quirion, Y. Tabuchi, A. Gloppe, K. Usami, and Y. Nakamura, Hybrid quantum systems based on magnonics, Appl. Phys. Express **12**, 070101 (2019).
[16] D. Xu, X.-K. Gu, H.-K. Li, Y.-C. Weng, Y.-P. Wang, J. Li, H. Wang, S.-Y. Zhu, and J. Q. You, Quantum Control of a Single Magnon in a Macroscopic Spin System, Phys. Rev. Lett. **130**, 193603 (2023).
[17] B. M. Terhal, J. Conrad, and C. Vuillot, Towards scalable bosonic quantum error correction, Quantum Sci. Technol. **5**, 043001 (2020).
[18] A. Kamra, W. Belzig, and A. Brataas, Magnon-squeezing as a niche of quantum magnonics, Appl. Phys. Lett. **117**, 090501 (2020).
[19] H. Y. Yuan, Y. Cao, A. Kamra, R. A. Duine, and P. Yan, Quantum magnonics: When magnon spintronics meets quantum information science, Phys. Rep. **965**, 1 (2022).
[20] D. D. Awschalom *et al.*, Quantum engineering with hybrid magnonic systems and materials (Invited Paper), IEEE Trans. Quantum Eng. **2**, 1 (2021).
[21] We emphasize the focus of this work on equilibrium squeezed magnons and their ground state vacuum (e.g., see [18,19,22–28]). These are qualitatively distinct from the squeezed states of magnons generated in nonequilibrium via some drives. There also exists much interest in and excitement about such nonequilibrium quantum states of magnons (e.g., see [19,29–33]).
[22] J. Zou, S. K. Kim, and Y. Tserkovnyak, Tuning entanglement by squeezing magnons in anisotropic magnets, Phys. Rev. B **101**, 014416 (2020).
[23] D. Wuhrer, N. Rohling, and W. Belzig, Theory of quantum entanglement and structure of the two-mode squeezed antiferromagnetic magnon vacuum, Phys. Rev. B **105**, 054406 (2022).
[24] J. Shim, S.-J. Kim, S. K. Kim, and K.-J. Lee, Enhanced Magnon-Photon Coupling at the Angular Momentum Compensation Point of Ferrimagnets, Phys. Rev. Lett. **125**, 027205 (2020).
[25] A. Kamra, E. Thingstad, G. Rastelli, R. A. Duine, A. Brataas, W. Belzig, and A. Sudbø, Antiferromagnetic

magnons as highly squeezed Fock states underlying quantum correlations, Phys. Rev. B **100**, 174407 (2019).
[26] H. Y. Yuan, S. Zheng, Z. Ficek, Q. Y. He, and M.-H. Yung, Enhancement of magnon-magnon entanglement inside a cavity, Phys. Rev. B **101**, 014419 (2020).
[27] V. Azimi Mousolou, Y. Liu, A. Bergman, A. Delin, O. Eriksson, M. Pereiro, D. Thonig, and E. Sjöqvist, Magnon-magnon entanglement and its quantification via a microwave cavity, Phys. Rev. B **104**, 224302 (2021).
[28] A. Kamra and W. Belzig, Super-Poissonian Shot Noise of Squeezed-Magnon Mediated Spin Transport, Phys. Rev. Lett. **116**, 146601 (2016).
[29] S. Sharma, V. A. S. V. Bittencourt, A. D. Karenowska, and S. V. Kusminskiy, Spin cat states in ferromagnetic insulators, Phys. Rev. B **103**, L100403 (2021).
[30] J. Zhao, A. V. Bragas, D. J. Lockwood, and R. Merlin, Magnon Squeezing in an Antiferromagnet: Reducing the Spin Noise Below the Standard Quantum Limit, Phys. Rev. Lett. **93**, 107203 (2004).
[31] J. Li, S.-Y. Zhu, and G. S. Agarwal, Squeezed states of magnons and phonons in cavity magnomechanics, Phys. Rev. A **99**, 021801(R) (2019).
[32] M. Elyasi, Y. M. Blanter, and G. E. W. Bauer, Resources of nonlinear cavity magnonics for quantum information, Phys. Rev. B **101**, 054402 (2020).
[33] M. Kounalakis, G. E. W. Bauer, and Y. M. Blanter, Analog Quantum Control of Magnonic Cat States on a Chip by a Superconducting Qubit, Phys. Rev. Lett. **129**, 037205 (2022).
[34] A. Kamra, U. Agrawal, and W. Belzig, Noninteger-spin magnonic excitations in untextured magnets, Phys. Rev. B **96**, 020411(R) (2017).
[35] K. Agarwal, R. Schmidt, B. Halperin, V. Oganesyan, G. Zaránd, M. D. Lukin, and E. Demler, Magnetic noise spectroscopy as a probe of local electronic correlations in two-dimensional systems, Phys. Rev. B **95**, 155107 (2017).
[36] S. Chatterjee, J. F. Rodriguez-Nieva, and E. Demler, Diagnosing phases of magnetic insulators via noise magnetometry with spin qubits, Phys. Rev. B **99**, 104425 (2019).
[37] B. Flebus and Y. Tserkovnyak, Quantum-Impurity Relaxometry of Magnetization Dynamics, Phys. Rev. Lett. **121**, 187204 (2018).
[38] S. P. Wolski, D. Lachance-Quirion, Y. Tabuchi, S. Kono, A. Noguchi, K. Usami, and Y. Nakamura, Dissipation-Based Quantum Sensing of Magnons with a Superconducting Qubit, Phys. Rev. Lett. **125**, 117701 (2020).
[39] F. Casola, T. van der Sar, and A. Yacoby, Probing condensed matter physics with magnetometry based on nitrogen-vacancy centres in diamond, Nat. Rev. Mater. **3**, 17088 (2018).
[40] Z.-X. Liu, H. Xiong, M.-Y. Wu, and Y.-q. Li, Absorption of magnons in dispersively coupled hybrid quantum systems, Phys. Rev. A **103**, 063702 (2021).
[41] Y. Tabuchi, S. Ishino, A. Noguchi, T. Ishikawa, R. Yamazaki, K. Usami, and Y. Nakamura, Coherent coupling between a ferromagnetic magnon and a superconducting qubit, Science **349**, 405 (2015).
[42] G. Burkard, M. J. Gullans, X. Mi, and J. R. Petta, Superconductor-semiconductor hybrid-circuit quantum electrodynamics, Nat. Rev. Phys. **2**, 129 (2020).
[43] A. Chatterjee, P. Stevenson, S. De Franceschi, A. Morello, N. P. de Leon, and F. Kuemmeth, Semiconductor qubits in practice, Nat. Rev. Phys. **3**, 157 (2021).
[44] M. M. Nieto, Displaced and squeezed number states, Phys. Lett. A **229**, 135 (1997).
[45] P. Král, Displaced and squeezed Fock states, J. Mod. Opt. **37**, 889 (1990).
[46] L. Trifunovic, F. L. Pedrocchi, and D. Loss, Long-Distance Entanglement of Spin Qubits via Ferromagnet, Phys. Rev. X **3**, 041023 (2013).
[47] I. C. Skogvoll, J. Lidal, J. Danon, and A. Kamra, Tunable Anisotropic Quantum Rabi Model via a Magnon-Spin-Qubit Ensemble, Phys. Rev. Appl. **16**, 064008 (2021).
[48] S. A. Bender and Y. Tserkovnyak, Interfacial spin and heat transfer between metals and magnetic insulators, Phys. Rev. B **91**, 140402(R) (2015).
[49] S. Takahashi, E. Saitoh, and S. Maekawa, Spin current through a normal-metal/insulating-ferromagnet junction, J. Phys. Conf. Ser. **200**, 062030 (2010).
[50] A. Kamra and W. Belzig, Magnon-mediated spin current noise in ferromagnet | nonmagnetic conductor hybrids, Phys. Rev. B **94**, 014419 (2016).
[51] See Supplemental Material at http://link.aps.org/supplemental/10.1103/PhysRevLett.131.143602 for (i) a detailed derivation of the system Hamiltonian and squeezing, (ii) a detailed derivation of the excitation energies, (iii) a detailed derivation of the effective squeezing between the excited state squeezed-magnon vacuum and the ground state squeezed-magnon vacuum, (iv) a description of the details of the numerical simulations as well as the simulation parameters, (v) examination of limits under which the qubit spectroscopy remains linear thereby probing the desired equilibrium superposition and how one can resolve the weaker peaks by employing larger Rabi drives, (vi) a discussion about the coherent coupling in the dispersive limit, and (vii) design equations for two different magnon-spin qubit platforms that admit direct dispersive coupling, which includes Refs. [52–65].
[52] T. Holstein and H. Primakoff, Field dependence of the intrinsic domain magnetization of a ferromagnet, Phys. Rev. **58**, 1098 (1940).
[53] N. N. Bogoljubov, V. V. Tolmachov, and D. V. Širkov, A new method in the theory of superconductivity, Fortschr. Phys. **6**, 605 (1958).
[54] R. Achilles and A. Bonfiglioli, The early proofs of the theorem of Campbell, Baker, Hausdorff, and Dynkin, Arch. Hist. Exact Sci. **66**, 295 (2012).
[55] I. I. Rabi, On the process of space quantization, Phys. Rev. **49**, 324 (1936).
[56] Y. Kajiwara, K. Harii, S. Takahashi, J. Ohe, K. Uchida, M. Mizuguchi, H. Umezawa, H. Kawai, K. Ando, K. Takanashi, S. Maekawa, and E. Saitoh, Transmission of electrical signals by spin-wave interconversion in a magnetic insulator, Nature (London) **464**, 262 (2010).
[57] F. D. Czeschka, L. Dreher, M. S. Brandt, M. Weiler, M. Althammer, I.-M. Imort, G. Reiss, A. Thomas, W. Schoch, W. Limmer, H. Huebl, R. Gross, and S. T. B. Goennenwein, Scaling Behavior of the Spin Pumping Effect in Ferromagnet-Platinum Bilayers, Phys. Rev. Lett. **107**, 046601 (2011).

[58] M. Weiler, M. Althammer, M. Schreier, J. Lotze, M. Pernpeintner, S. Meyer, H. Huebl, R. Gross, A. Kamra, J. Xiao, Y.-T. Chen, H. J. Jiao, G. E. W. Bauer, and S. T. B. Goennenwein, Experimental Test of the Spin Mixing Interface Conductivity Concept, Phys. Rev. Lett. **111**, 176601 (2013).
[59] L. Schlipf, T. Oeckinghaus, K. Xu, D. B. R. Dasari, A. Zappe, F. F. de Oliveira, B. Kern, M. Azarkh, M. Drescher, M. Ternes, K. Kern, J. Wrachtrup, and A. Finkler, A molecular quantum spin network controlled by a single qubit, Sci. Adv. **3**, e1701116 (2017).
[60] E. Lee-Wong, R. Xue, F. Ye, A. Kreisel, T. van der Sar, A. Yacoby, and C. R. Du, Nanoscale detection of magnon excitations with variable wavevectors through a quantum spin sensor, Nano Lett. **20**, 3284 (2020).
[61] J. R. Maze, P. L. Stanwix, J. S. Hodges, S. Hong, J. M. Taylor, P. Cappellaro, L. Jiang, M. V. G. Dutt, E. Togan, A. S. Zibrov, A. Yacoby, R. L. Walsworth, and M. D. Lukin, Nanoscale magnetic sensing with an individual electronic spin in diamond, Nature (London) **455**, 644 (2008).
[62] T. van der Sar, F. Casola, R. Walsworth, and A. Yacoby, Nanometre-scale probing of spin waves using single electron spins, Nat. Commun. **6**, 7886 (2015).
[63] K. Yang, W. Paul, S.-H. Phark, P. Willke, Y. Bae, T. Choi, T. Esat, A. Ardavan, A. J. Heinrich, and C. P. Lutz, Coherent spin manipulation of individual atoms on a surface, Science **366**, 509 (2019).
[64] L. M. Veldman, L. Farinacci, R. Rejali, R. Broekhoven, J. Gobeil, D. Coffey, M. Ternes, and A. F. Otte, Free coherent evolution of a coupled atomic spin system initialized by electron scattering, Science **372**, 964 (2021).
[65] T. Choi, W. Paul, S. Rolf-Pissarczyk, A. J. Macdonald, F. D. Natterer, K. Yang, P. Willke, C. P. Lutz, and A. J. Heinrich, Atomic-scale sensing of the magnetic dipolar field from single atoms, Nat. Nanotechnol. **12**, 420 (2017).
[66] Steven S.-L. Zhang and S. Zhang, Spin convertance at magnetic interfaces, Phys. Rev. B **86**, 214424 (2012).
[67] The ground state stability requires $A \geq 2|B| + \chi$, which yields a finite r_g.
[68] In contrast, the conventional qubit spectroscopy [10,11] of nonequilibrium superpositions yields peaks separated by the typically smaller quantity χ.
[69] J. R. Johansson, P. D. Nation, and F. Nori, QuTip: An open-source PYTHON framework for the dynamics of open quantum systems, Comput. Phys. Commun. **183**, 1760 (2012).
[70] J. R. Johansson, P. D. Nation, and F. Nori, QuTip 2: A PYTHON framework for the dynamics of open quantum systems, Comput. Phys. Commun. **184**, 1234 (2013).
[71] H.-P. Breuer and F. Petruccione, *The Theory of Open Quantum Systems* (Oxford University Press, New York, 2007).
[72] G. Lindblad, On the generators of quantum dynamical semigroups, Commun. Math. Phys. **48**, 119 (1976).
[73] V. Gorini, A. Kossakowski, and E. C. G. Sudarshan, Completely positive dynamical semigroups of N-level systems, J. Math. Phys. (N.Y.) **17**, 821 (1976).
[74] I. I. Rabi, Space quantization in a gyrating magnetic field, Phys. Rev. **51**, 652 (1937).
[75] Y. Tabuchi, S. Ishino, A. Noguchi, T. Ishikawa, R. Yamazaki, K. Usami, and Y. Nakamura, Quantum magnonics: The magnon meets the superconducting qubit, C.R. Phys. **17**, 729 (2016).
[76] D. Zueco, G. M. Reuther, S. Kohler, and P. Hänggi, Qubit-oscillator dynamics in the dispersive regime: Analytical theory beyond the rotating-wave approximation, Phys. Rev. A **80**, 033846 (2009).
[77] This can be done by, for example, employing a larger amplitude of the qubit drive since the qubit excitation increases with the drive [51].
[78] C. Ciuti and I. Carusotto, On the ultrastrong vacuum Rabi coupling of an intersubband transition in a semiconductor microcavity, J. Appl. Phys. **101**, 081709 (2007).